Progress in High-Energy Electron and X-Irradiation of Insulating Dielectrics

A. R. Frederickson
California Institute of Technology
Jet Propulsiom Laboratory
Mail Stop 303-217
4800 Oak Grove Drive
Pasadena, CA 91109, USA

Received 30 March, 1998

The effects of high-energy irradiation on the charging of insulators is reviewed primarily with a viewpoint similar to the seminal work of Professor Bernhard Gross. Recent results relating to insulation breakdown and to insulators in space radiation are more easily explained because of Gross' fundamental studies. A number of important issues remain unsolved, yet the first steps to solutions have been provided by Gross.

I Introduction

The works of Bernhard Gross, and our shared communications, have had a strong impact upon my work. His example has been a beacon of light as the years have passed and as we have explored some of the marvels of the natural world. The interest that he generates has expanded amongst his co-workers and a small community of scholars. When I meet someone who has worked with Professor Gross, the reaction is always the same - an immediate smile. If I have made progress, it has been due in part to the sharing of ideas with Bernhard Gross. His broad-ranging ideas in radiation charging were reviewed [1], and he even compiled literature references to help us [2]. The results that are reviewed here build upon [1] and other works of Gross, and have had useful application in spacecraft radiation problems.

In 1970, while measuring secondary electron emission and backscattering with high energy electrons incident on metal surfaces, I noted that some insulating materials and films were charging up to high negative potentials. Even dirty oxide surfaces of aluminum were charging to tens of millivolts (negative or positive depending on the dirt). The insulators were hidden from line of sight bombardment by electrons from the source and from the irradiated surface. But electrons nevertheless multiply scatter to eventually find their way into any insulators that were used to electrically isolate elements in the vacuum chamber. Once charged, the insulators remained charged until light was shone on them, or until the vacuum was eliminated by ingress of air. The electric fields produced by the trapped charges in the insulator altered the motion of low-energy electrons in the vacuum.

A search in the library quickly found the 1957 paper by Gross on the charging of borosilicate glass [3]. There he correctly laid out the basic ideas that are used to this day. Two-MeV electrons penetrate up to 0.4 cm into the glass. The distribution of penetrating electron-stopping depths combined with the divergence of thermalized carrier conduction currents were correctly identified as the sources of space charge and high electric fields in the insulator. The books by Bube and by Rose provided further insight to the electronic conduction process which Gross expanded upon [4] while analyzing the exact quantity and spatial distribution of charges stopped in the insulator.

Large Lichtenberg discharge figures were produced in the glass, as well as in the acrylic sheet, by the MeV electrons in Gross' studies. The formation of the discharge figure is accompanied by a brief pulse of current.[5] The time integral of the current pulse was found to be a significant fraction of the charge that had been stopped in the previously irradiated insulator. Since that time, every high energy radiation laboratory feels

compelled to make some of these fascinating Lichtenberg figures.

X-rays and Gamma rays are absorbed in material mostly by transferring energy and momentum to the electrons. A high-energy electron current is thereby produced that may also generate Lichtenberg discharge figures. Gross generalized this phenomena to develop the dielectric Compton Diode which generates a current proportional to the photon flux.[6,7] Vacuum diodes were in use [8], but currents of low-energy electrons in the vacuum complicated the results. The dielectric had the advantage of suppressing currents of low-energy electrons while the high-energy electrons would traverse one electron range in the dielectric.

II Improvements on the box model

The ideas in the early work of Gross were general. But the first experiments were necessarily related to theoretical models that were analytically tractable. The box model was a simplification that proved to be very profitable, especially with monoenergetic electron beams which partially penetrated the insulator [9,10]. In the box model it is assumed either that all electrons penetrate to the same stopping depth, or that an average stopping depth is sufficient to model the problem. In the depth penetrated by electrons, conduction is dominated by radiation-induced mobile electron-hole pairs. In the depth beyond electron penetration, conduction is dominated by normal dark conductivity and by charge injected from the irradiated region. The box model and related experiments showed that the dominant processes involved the stopping of the primary electrons, the generation of static electric field by the stopped electrons, the generation of electron-hole pairs in the conduction-valence bands, and the development of conduction currents proportional to the product of local electric field and electron-hole concentrations.

Once the box model had proven the basic concepts, it became possible to provide computer simulation for the more general problem. Gross proposed a semi-analytic model which required computer solution of integrals [11]. Independently, and nearly simultaneously, several groups produced straightforward computer simulations of the one- dimensional problem [12-16]. This simulation technique, developed by many, will henceforward be called NUMIT (for numerical iteration). In the NUMIT simulation one can calculate the full time- and space-complexity of stopped charge, field, and conduction currents. The simulation allows one to rapidly change many parameters for comparison with experimental results. For example, one may include the dependence of conductivity on electric field, or on accumulated radiation dose, both of which had been mentioned by Gross in his early work. In general, NUMIT allows for easy inclusion of the dependence of any parameter, such as conduction current, on any of the other parameters, such as electric field and irradiation dose. NUMIT allows for time and spatial dependent injection, diffusion, effects of trapping, spatially and time varying trap concentrations, and can include the effects of steep doping profiles to simulate semiconductor junction behavior.

The problem can be described mathematically in a simple fashion. Since mathematical detail is not necessary in this review, the one-dimensional model is simplest to envision. Radiation generates a current which subsequently stops in, and charges, a dielectric. Electric fields develop conduction currents, and the conduction charges are provided by any source including photogeneration of electron-hole pairs, thermal generation, field-induced tunneling from traps, electrode injection, etc. The separation between high- energy particles and conduction processes in the thick materials considered here can be arbitrary. Usually particles above 100 eV are considered primary particles, and all below 100 eV are tracked as either stopped or as conduction particles. The complex reasons for this are left unsaid. The general equations are thus: The charged particle current is the sum of three independent terms,

$$J_p = J_{\rm fas} + J_{\rm conduction} + J_{\rm diffusion}. \qquad (1)$$

The differential equation for space charge density is

$$\frac{\partial \rho(x,t)}{\partial t} = -\frac{\partial J_p(x,t)}{\partial x} \ . \qquad (2)$$

The electric field is found from solution of

$$\epsilon \frac{\partial E(x,t)}{\partial x} = \rho(x,t) \ . \qquad (3)$$

subject to the boundary conditions and added to any externally applied electric field:

$$\int_a^b E(x,t)dx = V_{app}(t) \ ; \qquad (4)$$

$$J_{\rm total}(t) = J_p(x,t) + \epsilon \frac{dE(x,t)}{dt} \ , \qquad (5)$$

where a and b are the positions of the electrode-insulator interfaces, and V_{app} is the applied voltage. As in Gross' box model, this system is quasistatic and neglects the (small) effects of magnetic field.

III Progress at high electron energies above 10 keV

1. Analytic and Monte Carlo Determination of Electron Stopping Depth Distribution.

Stopping of electrons is often the primary process for charging insulators or insulated material. Calculation of the distribution of stopping depths of electrons is essential for modeling the charging process. Gross provided an early measurement of depth distribution for dielectrics [17], and such problems were also addressed by radiation transport work in the nuclear industry [18]. Gross et al provided further measurements for direct application in the electret field with electrons from 10 to 50 keV [19].

Tabata, Andreo and Ito [20] have used the widely available Monte Carlo codes [21] from the nuclear radiation field to tabulate stopping depth for normal incidence electrons at many energies from 100 keV to 100 MeV in nearly any material. A number of experiments have confirmed the Monte Carlo electron transport codes for specific cases. An analytic function is available [22] which fits the tabulation [21] within a few percent for both current transmission and stopping depth distribution at all energies from 100 keV to 100 MeV. The analytic function interpolates between the electron energies and material atomic numbers tabulated by Tabata and Ito, and thereby covers a broad range of energies and atomic numbers.

2. Effect of Space-Charge Fields on the Transport of Fast Electrons.

In material, the slowing of fast electrons acts as if there were an electric field continuously decelerating the electron. In solids, the slowing is produced by an effective decelerating field of approximately 2 MV/cm for electrons of energies from 300 keV to 3 MeV. Yet it is possible to sustain space charge fields of 2 MV/cm for minutes to hours without breakdown of the solid dielectric. It becomes obvious that the largest space-charge field will at least slightly alter the motion of the high-energy electrons while inside the dielectric. This had been cleverly analyzed for specific cases [23,24], but full inclusion of the details of the three-dimensional motion of the electrons for any material and geometry was beyond analytic solution. Inclusion of the effects of electric field in Monte Carlo transport simulation provides the general solution of the problem.

Modeling of irradiations with electrons below 50 keV can usually ignore this effect. At 10 keV, the electron stopping field is at least 20 MV/cm in typical solids, well above the sustainable static electric field. Nevertheless, the calculational method was developed and tried at 20 keV where the electron motion could be described classically [25]. The calculations found no effect, less than 1% change in depth of penetration in a thick slab. For the purpose of mathematical modeling, the density of the dielectric can be made arbitrarily small so that the stopping power vanishes while the space-charge field remains large. But experimental verification below 50 keV awaits the development of low-density solid insulators (which seems impossible). With such insulators, one might measure the space charge and internal electric field distributions by any of the methods reviewed by R. Gerhard-Multhaupt [26].

Hikita and Zahn provided the impetus to extend the calculation of fast electron trajectories with electric fields to relativistic electron velocities. They measured the time and depth dependent evolution of space-charge electric fields in thick polycarbonate with partially penetrating 2-MeV electrons [27]. In these measurements, the zero-field plane was found to move towards the irradiated surface as time progressed. However, if the electric field does not act on the fast electron trajectories, then the zero-field plane should move away from the irradiated surface [28]. By combining the field-dependent trajectories of the fast electrons with the NUMIT simulation, and by including high-field conduction effects, the experiments of Hikita and Zahn were correctly modeled [28]. Gross outlined the utility of the concept of the zero-field plane [29] which assists one to interpret experimental results.

Irradiation of plexiglass and polycarbonate produces darkened regions where the fast electrons have passed [2]. Inspection of this discolored layer indicates that it is substantially thinner than the maximum penetration of fast electrons in the absence of space-charge fields. Here was direct evidence that internal fields were foreshortening the range, but it was not studied in the literature. [Soviet Union publications in the 1970s and

80s hinted that such work was progressing, but disclosure was limited leaving the exact results unclear.] Figure 1, taken from [28], indicates how the experiments of Hikita and Zahn allowed the model to be developed to include correct charge penetration, dose penetration, and conduction physics. Experimental measurement of electric field in high-energy irradiations is a key ingredient to further progress.

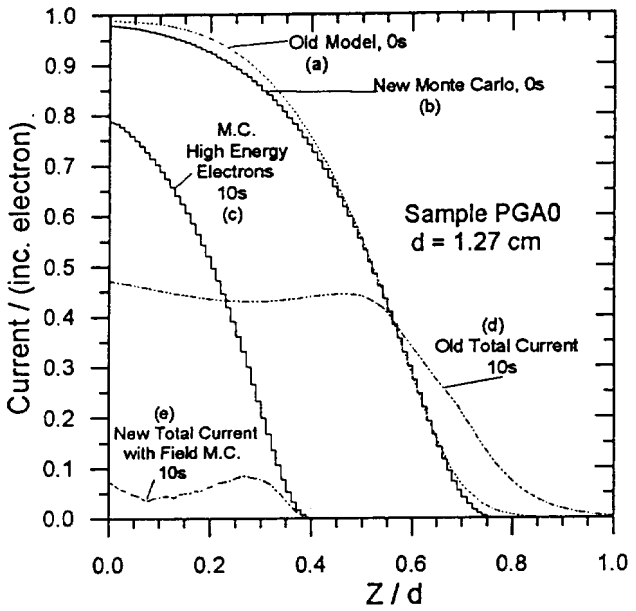

Figure 1. Comparison of Field Dependent Monte Carlo (M.C.) Simulation with Earlier (Old) Field- Independent Simulation. The high-energy electron current penetration after ten seconds of irradiation: without field dependence is given by (a) or (b), and with field dependence is given by (c). The total current at ten seconds including conduction processes is given by: (d) with field-independent fast electron transport, and (e) field-dependent fast electron transport. At ten seconds the electric field strength was of order MV/cm, and other details are in [28].

3. Secondary-Electron Yield from Dielectrics as a Function of Electric Field.

Simulation, such as NUMIT, can be used to model many details within an experiment, including secondary electron emission. Consider a dielectric slab with thin metal foils painted on both sides of the dielectric. Assume that NUMIT correctly determines the currents of high-energy electrons, radiation-induced conduction currents, space-charge distribution and electric fields in the insulator under bombardment by high-energy electrons [27,28]. One can perform the experiment and the simulation by choosing the incident electron energy such that a small fraction of the electrons pass completely through the insulator. The current of through-penetrating electrons, as well as their dose in the following material, can be measured as a function of time while electric fields build up in the insulator. Usually, the fraction penetrating and their dose will decrease as time progresses and the dielectric accumulates space charge [27,28]. NUMIT seems to correctly simulate all of the details in this irradiation, including field dependent conductivity in the insulator near the electrodes.

Consider the arrangement of Fig. 2 where the first irradiated metal foil is separated from the insulator by a vacuum space of any chosen distance, say 1 cm. In the planar one- dimensional geometry, the act of separating the foil causes the following changes (all of which are included in a NUMIT simulation):

1) Secondary electrons, which are conduction band electrons escaping the insulator, will accelerate away from the negatively charged insulator and enter the first metal foil. 2) The high-energy irradiation electrons will be slowed by the electric field that is generated in vacuum between the foil and the insulator, and therefore fewer electrons will completely penetrate the insulator. Both the field in the vacuum and the field in the insulator will reduce the dose rate behind the insulator. Choosing a thick vacuum causes the field in vacuum to reduce the penetrating dose more than the field in the insulator reduces the dose. 3) The current monitored between the electrodes is proportional to the distance traveled by each charge carrier [30]. Conduction electrons in the insulator move only short distances before being trapped, perhaps one micrometer or less. But conduction electrons in the vacuum move entirely across the vacuum, 1 cm, and thereby contribute large current between the electrodes.

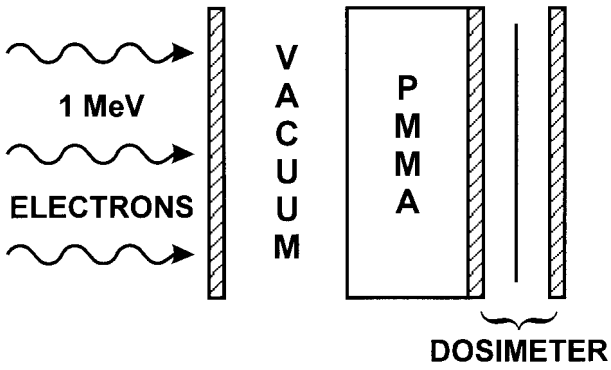

Figure 2. Experimental Arrangement for Measurement of Field-dependent Secondary Electron Emission by Irradiated Insulator (polymethylmethacrylate).

Thus, the contribution of secondary electron current to the total electrode current becomes large for

thick vacuum and its effects will be clearly seen in the experiment and in the simulation.

The experiment to measure secondary electron emission proceeds as follows. First, an experiment is performed with the first electrode painted on the insulator, and the parameters of the simulation are found to correctly predict the time dependent foil currents and penetrating dose. This establishes the correct insulator-dependent parameters for calculating the radiation-induced currents, conduction and electric field in the insulator. Second, the first foil is displaced from the insulator in vacuum, and the same electron irradiation is performed on a virgin sample. The effect of the vacuum field must be included for simulating the trajectories of the irradiation electrons. As the simulation proceeds through time, the secondary electron current across the vacuum is adjusted so that both the calculated electrode current and the calculated penetrating dose rate are in agreement with the measured time-dependent current and dose rate. Within the simulation is the time and position dependent electric field, including the field at the vacuum surface of the insulator. Thus, at each time, one has determined the surface electric field and the secondary electron current, and thus the dependence of secondary yield on electric field at the sample surface.

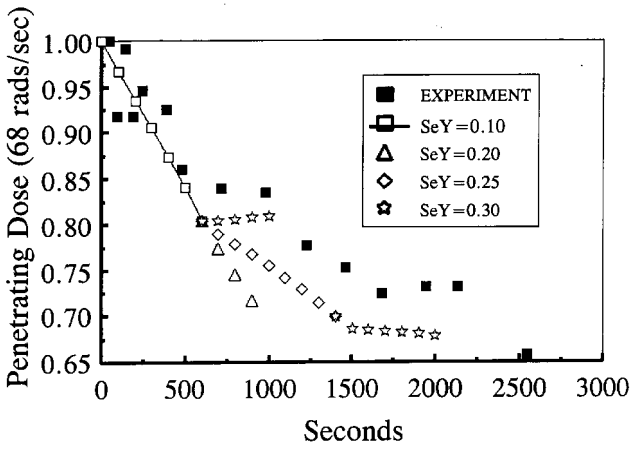

Figure 3. Simulation of the Effects of Secondary-Electron Yield, SeY, on Field Build-up and Dose Penetration.

The results for polymethylmethacrylate using 1-MeV electron tests are commented [31] where the secondary yield increased roughly a factor of ten for electric fields of roughly 30 kV/cm. Fig. 3 indicates how the simulation models the experiment. With zero field, the secondary yield is roughly 2%, and the simulation successfully reproducess the experimental data for 500 seconds using secondary yields of 2% to 10%. After 500 seconds, the simulation must use a secondary electron yield of 25% to reproduce the experimental result. After 1500 seconds the secondary yield must again be increased so that the simulation reproduces the experiment.

4. Relationship Between Pulsing and the Space-charge Electric Fields.

One can monitor currents between the electrodes for the occurrence of pulsed discharges. The NUMIT simulation of the conditions of the irradiation will determine the electric field at the time of the pulsed discharges. This has been reviewed [32], and two examples are indicated in Figs. 4 and 5 with electrodes attached to both surfaces of the planar insulators under partially penetrating electron beams. In clear sheet stock without obvious flaws the pulses are infrequent. In fiberglass-filled material the narrow glass fibers apparently induce frequent pulses. In all materials tested, the pulsing did not occur until the field strength was above 100 kV/cm.

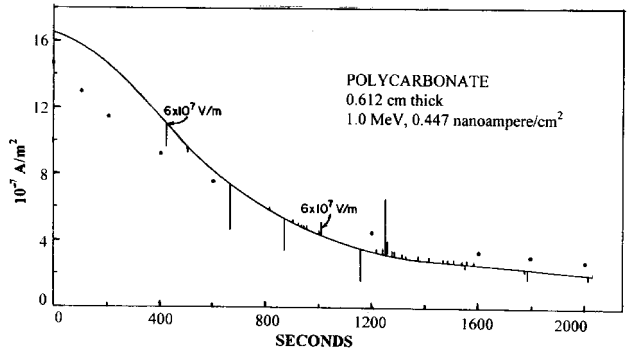

Figure 4. Simulation and Experiment in Clear Polycarbonate. Simulation provides the series of dots. Experiment provides the continuous chart recorder trace of the current to ground from the rear electrode. Vertical spikes are caused by small partial discharges in the insulator. The electric field reaches pulsing magnitude at the front electrode at 400 seconds, and at the rear electrode at about 900 seconds.

Inside the solid material, each pulse reduces only a tiny portion of the electric field in the insulator. Inside fiberglass-filled insulators, pulses will continue for several days after the radiation is turned off. Although discharges do not alter much of the electric field inside the dielectric, when a vacuum space exists between the first electrode and the insulator surface, the current pulses across the vacuum are very large, and the electric field in the entire vacuum space is substantially reduced by a single pulse [31,33-35]. The fact that the vacuum fields

are largely reduced by a single pulsed discharge process [35] is the origin of the pulse scaling laws [33].

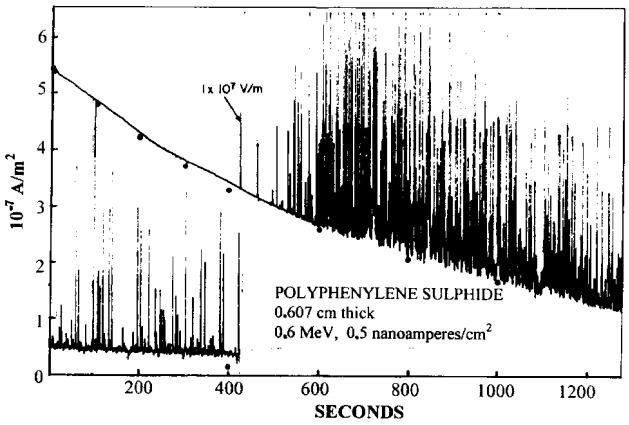

Figure 5. Simulation and Experiment in Fiber-filled Material. The simulation (dots) follows the experiment, but the pulsing frequently drives the chart recorder off scale. The second trace is the same experiment at later times, and indicates that pulsing is less frequent despite the fact that fields have increased. Pulsing continued several days after the electron beam stopped. The first pulse occured when the electric field was 1×10^7 V/m.

5. Effect of Fast Electrons on Spacecraft Insulation

The flux of space radiation is dominated by fast electrons. Typically, one to two mm of aluminum shielding is provided to protect the electronics by reducing the intensity of the radiation. This has the effect of stopping electrons below perhaps 700 keV, but allows the less populous electrons above 1 MeV to penetrate into the electronic circuits. The total dose to electronic devices is reduced to an acceptable level, but the insulating materials eventually develop high space-charge electric fields as stopped electrons accumulate.

Analogous to the Lichtenberg discharges investigated in glass and plexiglass [1,2], the spacecraft insulators produce discharge pulses that can interfere with electronics by producing 100-volt pulses on circuit-board traces [36]. Pulsing of insulators has been correlated with operational problems on spacecraft [37]. Figure 6, taken from [38], indicates the rate at which several insulating materials pulsed during 14 months in Earth orbit. The pulse rate is proportional to a power of the high-energy electron flux [39]. Insulators with fiberglass filler pulsed [38] most frequently, probably due to the electric field enhancement at the ends of the fiberglass. TFE based insulators pulsed most frequently during the first months in orbit because accumulated radiation on TFE increases the dark conductivity thereby reducing the electric field in later months [40]. FR4 fiberglass-filled circuit-board pulsed most frequently after several months, probably because outgassing for several months reduced the dark conductivity. Pure sapphire never pulsed, perhaps because it has a large carrier schubweg, or high radiation-induced conductivity. Clear FEP Teflon pulsed occasionally.

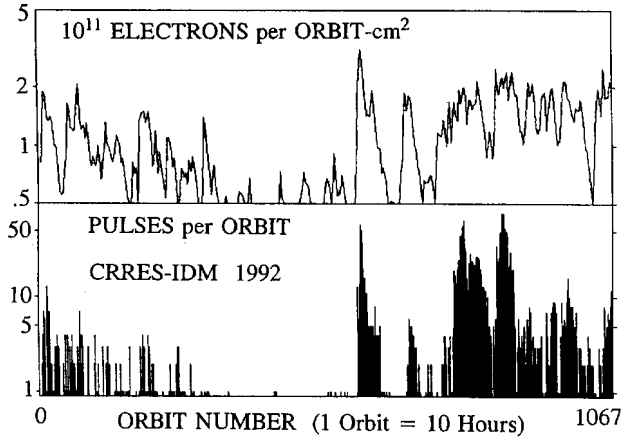

Figure 6. Pulse Rate Summed Over All Insulators Monitored in Space for 14 Months Compared to Fast Electron Flux.

It is tempting to predict that a pulse will occur when the voltage, or the electric field, achieves a particular level during the space radiation. But this simple model, although appealing, does not work. Instead, as the electric field grows, some pulsing occurs while the electric field continues to grow. Eventually the electric field will reach a maximum, and the rate of pulsing is likely to decline while the maximum field is maintained [32]. In some samples, the pulse rate declines to nearly zero. I remember discussing this with B. Gross 15 years ago when he related it to the phenomena of self healing in high voltage capacitors. The space test results [38] are very similar to the ground test results [32], and are probably related to Gross idea about self healing.

The pulsing data from a space experiment can be used to help spacecraft designers predict the rate of pulsing that might occur at insulators inside a spacecraft [39]. There is little other data to help one predict the rate of pulsing. The measured pulse rate was found to relate to a power of the high-energy electron flux. Pulse monitors are rarely flown on spacecraft, and the fundamental measurement of pulse rate is rarely available. When spacecraft have problems, and the space electron radiation is simultaneously enhanced, it is appealing to blame the radiation-induced ESD pulsing for

causing the problems. Yet proof of pulsing is almost always lacking. On one spacecraft a significant percentage of approximately 400 problems in several instruments occurred simultaneously (time resolution in the spacecraft data stream was 32 seconds) with a large ESD pulse observed by a pulse detector inside a different instrument [37]. Thus, it was proven that ESD pulses were the cause of numerous problems on this spacecraft. Usually, lacking actual pulse measurement, one only infers (not proves) that ESD pulses caused problems if the problems occurred when the exposure to high-energy electrons is elevated.

6. Charging of Spacecraft Relative to Plasma Potential

At the surface of the spacecraft, the space radiations can charge the entire spacecraft relative to the ambient plasma potential. Spacecraft surface potentials vary from a few volts positive to 20 kV negative [41,42]. The surface potential is measured using electron and proton spectrometers which detect the acceleration of the normally cold (1 eV) plasma particles. Secondary electron emission [43] and photoemission from surfaces of the spacecraft usually prevent high negative charging. Occasionally, spacecraft experience a high flux of electrons above 10 keV which overwhelms the secondary electron and photoelectron currents and negatively charges the spacecraft [41]. Different potentials between isolated portions of the spacecraft can exceed 2 kV [44] and produce electrostatic discharge pulses that interfere with spacecraft circuits [45]. A spacecraft design standard has been in use for a decade to help designers prevent problems from the charging of outer spacecraft surfaces [46].

7. Discharge Pulse Scaling Laws, and Pulse Shapes.

An extensive early set of experimental data were summarized as pulse scaling laws [33]. This work was mostly performed with electron beams at ten or twenty keV, although some work with higher energy electrons from a radioactive source found similar results. Subsequently, others found similar results when their tests were also performed in small conductive vacuum chambers. Still others found different pulse shapes when testing in much larger chambers, or with differently structured samples. Much of the pulsing data has been recently reviewed, and it is proposed that nearly all pulse shapes can be related to a single process [35,34].

A pulse begins with a small discharge internal to the insulator similar to the Lichtenberg tree phenomena. For low-energy electron beams, it may be a surface Lichtenberg tree. Or, it could begin as the explosion of a dielectric needle at its surface stressed by high electric field. Each of these phenomena issues a burst of partially ionized gaseous matter into the vacuum which evolves into a gaseous discharge. The gas discharge evolves and compensates the voltages on the surfaces exposed to the vacuum-gas discharge medium. The current which flows in the gas discharge produces the measured signals that form the scaling laws and the pulse shapes reported in the literature.

The gas discharge expands in the vacuum at thermal gas velocities to electrically short-circuit electrodes that are biased by power supplies, solar cell arrays, or batteries. More than 100 amperes can be conducted with only 100 volts applied from batteries [34]. The amount of gas evolved, the rate at which it expands into vacuum, and the current waveforms have been investigated [34]. Since the gas can short electrodes differing by only 100 volts, it will certainly short together spacecraft surfaces that have voltages differing by a kV or more, and gaps of 20 cm have been spanned [Fig. 7 in 35]. It appears that the pulse shape is partly controlled by the evolution of charge currents in the gaseous discharge.

8. Application to Vacuum Electron Tube Glass Envelope Breakdown

Vacuum electron tubes were usually contained in a glass envelope, and discharges of the glass were not reported. Yet high-energy electron beams on glass quickly produce discharge pulses [3]. Why was this not seen in vacuum electron tubes?

Almost always, electron tubes were operated with the cathode near ground potential. The glass envelope remained near ground potential and did not exhibit effects of static charge (unlike television picture tubes and computer monitors which are obviously charged and attract dust, etc.). The anode of the tube was at high positive voltage. Thus, electrons would bombard the glass envelope only at thermal energies, not at high energies. It was unlikely for the glass to charge more than a few volts.

But high voltage can be applied across the glass envelope by operating the cathode at high negative potential. A metal shield might be placed around the

outside of the glass envelope. Electrons from the cathode might bombard the glass and ultimately apply the full cathode potential across the glass. Vacuum tube glass envelope breakdown has been reported [47].

9. Failure of Insulation with High-Energy Radiation at Moderate Flux.

Irradiation produces enhanced conductivity [1,4] and Lichtenberg discharge trees [3,5] in the insulators. In most insulators the conductivity current is small, usually no larger than the current carried by the radiation itself. However, the conductivity current in photoconductors is large and this effect is used to detect radiation. Usually, the Lichtenberg discharge trees do not penetrate the insulator. The discharge tree weakens the insulation only to the extent that a thin hole drilled in the insulation weakens it. The tree forms instantly in one burst and does not seem to produce the tracking phenomena that repeated discharges are known to produce in high voltage power supplies. Can the radiation cause insulation failure?

Complicated arrangements of material can bring together various effects with disastrous results. Obviously a photoconductor, made sufficiently conductive, will overheat upon application of sufficient external bias. Recent experience in space and in ground tests indicates that the radiation-induced effects can cause insulation failure that was not predicted. Although not a photoconductor, kapton slowly pyrolizes under radiation, including uv, to become more conductive, especially at elevated temperature in sunlight in space. A radiation-induced discharge by fully insulating material can initiate a current flow in nearby electrodes under battery bias [34] to induce a continuous glow discharge. The glow discharge can initiate local heating of kapton which pyrolizes to become permanently conductive. Even if the glow discharge is stopped, the conductive kapton will overheat under resumed bias to eventually form a carbon electrical short [49]. Spacecraft solar arrays with kapton operating above 50 volts have failed. Rearrangement of materials and electrodes can prevent such problems [50].

Immediate failure of the insulation upon formation of the radiation-induced discharge tree has been reported [51]. With certain arrangements of irradiation and applied bias, the radiation-induced discharge tree can be made to propagate entirely through the insulator to form a conducting channel of gaseous plasma between biased electrodes. The short circuit will remain as long as the power supply provides enough energy to continue evolution of gas from the electrodes and nearby insulation.

Cosmic rays impinging thin insulation in modern microcircuits have been implicated in insulation failures. Microcircuits are typically operated at ten volts and less. The cosmic ray induces a high level of conducting electron-hole pairs in a submicron tube surrounding its track. Whether this tube can devolve into a breakdown, or simply appears as a transient space-time spike of conductivity is a subject of controversy. The studies reviewed in this paper are at low levels of ionization, with high voltage, and cannot contribute to resolution of this problem.

10. Another Compton Diode and Radiation Detector.

High-energy X-rays and gamma rays passing through material develop a forward moving flux of fast electrons. The divergence of this current deposits charge in the material. The total charge deposited is therefore proportional to the attenuation of the photon current [6,7]. The basic Compton Diode as discussed by Gross, therefore, produces a current which cannot exceed the initial photo-Compton electron current produced by the photons upon passage through one electron range in the material.

Another configuration of material produces greater total current from the same photon flux [48]. This configuration was determined by consideration of the details of the photo-excited and Compton-generated electron transport processes in multi-layer structures. The electron current produced in low atomic number material, say Be, greatly exceeds that in high atomic number material, say Pb. This is caused by strong nuclear scattering in the Pb which decreases the forward motion of electrons. Consider a bilayer material, Be-Pb, with photons incident on the Be first. Electrons entering or generated in the Be mostly move forward and are either stopped in the Pb, or scattered back from the Pb to be stopped in the Be. Thus Be-Pb absorbs many electrons and emits few. Next, consider Pb-Be. Electrons entering or generated in Pb are likely to be scattered back out of the Pb, and electrons entering or generated in the Be are likely to pass through and exit the Be. Thus Pb-Be absorbs few electrons and emits many. Therefore, an electrode consisting of Be-Pb will accumulate electrons from surrounding material, and

an electrode consisting of Pb-Be will emit electrons to surrounding material.

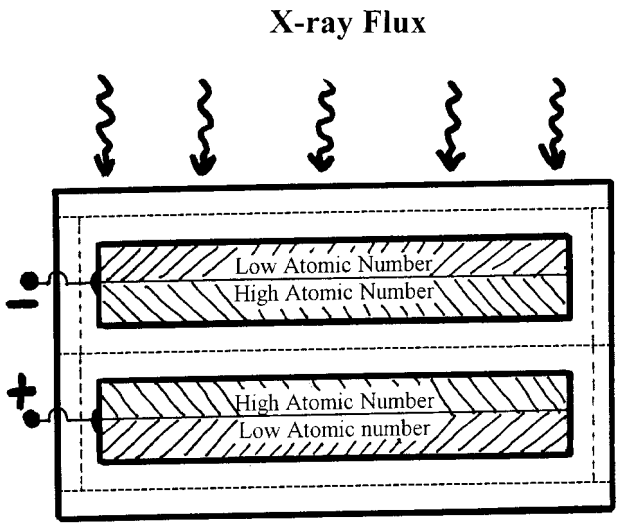

Figure 7. Arrangement of Conductors for an Efficient Compton Diode Cell. The dashed lines (—) indicate insulator foils to block low energy electron currents.

One can alternately stack many planar Be-Pb electrodes with many planar Pb-Be electrodes to form a battery by passing gamma rays through the stack. The Be-Pb electrodes can be connected together to form the negative current source, and the Pb-Be can be connected together to form the positive current source. The total current generated can exceed that generated by the elementary Compton Diode, provided a reasonable choice of Be and Pb thicknesses are chosen [48]. Series wiring of these cells can achieve high voltage, provided that secondary electron current between cells does not counter the development of high voltage. One can prevent secondary electron currents by interjecting thin insulator materials between the electrodes. It is certainly unusual to improve a battery by surrounding its electrodes with insulation! The thin insulators pass the high-energy electron currents which provide the electromotive force for the cell, and prevent the low-energy electron currents which tend to deplete the cell power.

It is instructional to think of the cell in this fashion. The full Compton current is developed in only one electron range of material. But very little of the gamma rays are attenuated in one range of material. If the electron current generated in the first electron range is abstracted for use, then nearly the same amount of current can be generated and abstracted from the second electron range of material, and the third, etc. The proper arrangement of high- and low- atomic number material best approaches this ideal cell arrangement. Although patented [48], I do not know if this device is being used anywhere.

IV Future work enabled by past successes

1. Analysis for Non-Normal Incidence.

Analytic functions fit to fast electron current penetration for non-normal incidence now seem possible. Although the functions for normal incidence appear complicated, they are actually based on simple concepts [22]. For non-normal incidence, one needs to modify the normal incidence concepts with the following ideas. A small fraction of off-normal electrons will be scattered by the first several atomic layers near the surface to be essentially normal incidence. Thus, the deepest possible penetration will be the same as for normal incidence. The fraction backscattered out of the surface and the fraction stopped at shallow depth will increase monotonically with angle of incidence. The fraction stopped at deep depth, and the average depth of penetration will decrease monotonically with angle of incidence. The actual quantitative dependencies should be determined by applying the Tiger codes [21] to non-normal incidence perhaps in ten-degree intervals, with smaller intervals from 70 to 90 degrees.

Secondary electron yields are proportional to dose rate in the first 50 angstroms for metals, 1 micrometer or more in insulators. Conduction and electron-hole pair production are proportional to dose rate at every point in the insulator. Thus, the on-going models by Tabata and co-workers for dose rate as a function of depth for non-normal incidence should be adapted to our insulators.

2. Total Insulation Failure Under High-Energy Radiation.

The conditions under which insulation fails are not well characterized. How do Lichtenberg trees or other pulsed discharge processes pass entirely through the insulator? How much gas is evolved during the pulsed discharges, and how large is the gap that can be spanned as a function of applied electrode bias? Can discharge trees be prevented? Does radiation induce special aging problems? These and other questions are important for the ultimate design of improved insulation.

Ground tests for ESD pulsing caused by 10 to 50 kV electron irradiations have been interpreted to indicate that a discharge-related stream of current has passed completely through the insulator [52]. This interpretation resulted from observation of pulses of negative charge flowing to ground from the rear electrode, simultaneous with decay of the negative voltage on the floating front surface of the insulator. It was sometimes stated that electrons punched through the sample from near the front surface.

In performing similar experiments, Levy was able to prevent this polarity of pulse by completely covering the rear electrode with insulator [34]. I interpret this to mean that negative pulses propagate to the rear electrode during the gaseous discharge process by going around the edge of the insulator sample. The front surface may not discharge by punch-through of the insulator. By blocking the gas from accessing the rear electrode, one blocks the discharge from proceeding to ground via the rear electrode. When so blocked, the discharge of the front surface must proceed by negative charges flowing away from the floating surface, and away from the rear electrode, and towards the electron gun, resulting in positive (image) charge flowing from the rear electrode to ground. Our experiments [34] proved that, in our tests, punch-through did not occur.

The general question remains: under what conditions can electron irradiation cause breakdown of insulators between electrodes, including punch-through breakdown.

3. Field-Dependent Conduction and Emission.

Conduction and secondary emission are strongly dependent on electric field. This creates a problem in analysis at the surface of insulators. The conduction current that escapes the surface to become secondary electrons generates significant positive charging within a depth of one schubweg below the surface. This requires the NUMIT to model conduction with a fine depth resolution near the surface. For thin insulators, less than 100 micrometers, electron emission and field-dependent mobility become very important parameters. These facts are already well known in radiation effects in silicon dioxide passivation in microelectronics, but NUMIT simulation has not been performed in these applications.

4. Nature of the Discharge Pulses.

Are the ESD pulses in irradiated insulators similar to the pulses in DC-biased capacitor dielectrics? Certainly, the electric field plays a dominant role as causitive agent in irradiated insulators. But if we had applied the same electric field using batteries, would the statistics of pulsing have remained the same? Or does radiation modulate the processes of pulse formation so that the same E-field in irradiated insulators makes more frequent pulses, or a different ratio of number of large pulses to number of small pulses? Until these questions are answered, one cannot use high voltage alone to test for pulsing in irradiated dielectrics, one must use radiation in reasonable simulation of the in-service radiation.

For example, it is suspected that the fiberglass filled materials pulsed frequently because the fields at the tips of the fibers became enhanced and initiated frequent pulses [53]. Radiation alters the conductivity of materials. If the fiber material becomes more conductive while the base material remains constant, the pulse rate will be increased. But if the fiber material remains constant and the base material conductivity increases, then field enhancement and pulse rate will both decrease.

5. Discharge-Pulse Scaling Laws.

The discharge-pulse scaling laws were empirically determined using electron beams of 10 kV to 20 kV where irradiated surfaces charge to roughly 10 kV. A single pulse discharges a significant portion of the surface voltage over most or all of the surface area. But inside a metal box under electron radiations above 100 kV at space intensities, the discharge pulses did not continue scaling to higher amplitude. Instead, the pulse amplitudes on 50 ohm transmission lines did not exceed 100 volts, and the total charge did not alter the surface voltage more than a few hundred volts [55]. At high intensity 1 MeV irradiation, however, the pulses did attain significantly higher amplitude than with the 20 kV irradiations [31].

It is tempting to presume that low fluxes allow charge to leak away through dark conductivity before high voltage is achieved. But this means that the electric fields would be small and pulsing would be unlikely. Unexpectedly, pulsing is seen in space on samples of 3 mm thickness at apparently less than 1 kV surface voltage. Much more study is needed for application of scaling laws on spacecraft.

6. Contact Effects.

High-energy irradiations are often concerned with thick samples and high space-charge voltage. The issues of blocking contacts are diminished because extreme electric fields can be generated to force conduction across the contact, because radiation-generated carriers cross the contact before being thermalized, and because the voltage generated at the blocking contact is small relative to the voltage generated across the thick insulator. Yet the issues remain important, and the work begun by Gross and others for thick insulators [1,4,9,11,43,54] should be continued.

7. Radiation-Induced Point-Defect Introduction Rate in Insulators.

Defects are introduced into the silicon lattice by electrons above 300 keV. The rate of atomic displacement rises rapidly as electron energy is increased. At these energies, collision can impart enough energy to cause a silicon atom to move at least one atomic spacing to occupy an interstitial position. The energy of displacement is related to the binding energy between neighboring atoms. By comparing experiments using electrons below 100 keV with experiments using electrons above 1 MeV, it might be possible to measure the effects of displaced atoms on the conduction processes in highly insulating dielectrics.

The fast electron has the advantage of generating electron hole pairs in the conduction/valence bands in known quantity for fast electron energies above 100 eV. The electron-hole excitation process is optical and differs only in rate, not in kind, as the primary electron bombardment energy varies. Defects introduced by electron irradiation above 1 MeV may act as conduction electron or hole traps to reduce the conductivity of the insulator so that it better stores charge. Irradiations below 0.1 MeV will not directly introduce defects as readily. Comparison between the two irradiations might indicate an effective rate of trap introduction by MeV electron bombardment. It is conceivable that insulators in extended use in space will be so altered in their charge storage properties, or practical insulators can be modified to useful advantage. Space measurements have indicated aging of charge storage properties, but the cause is uncertain [38].

8. Conduction Processes.

Gross and co-workers have provided many examples of the effects of various conduction processes on the charging of insulators. As new samples are tested, these and other effects are sure to be important, and for real applications one must carefully consider the processes of conduction. The papers by Gross on radiation-related conductivity provide useful guidelines for interpretation of future insulator irradiation experiments. This review emphasized the high-energy aspects, not mechanisms of conductivity. But full understanding of real data requires information on the conductivity processes. In various situations I have had to apply conduction models involving: percolation, electrode injection, hole transport, H, OH and O radicals, polarization, multiple trapping levels, diffusion, etc. However, the level of conductivity in these experiments usually is exceedingly low, high field effects often are important, and the mechanisms invoked to explain the results are easily disputed because the experimental data are sparse while conduction phenomena are certainly numerous. Conduction phenomena are best studied in a large array of literature beyond that reviewed here.

V Summary

This paper revews the progress in understanding of electrical current and electrostatic charging, and their effects, in insulators irradiated by high energy particles and x-rays. Much of the progress is based on the works of Professor B. Gross. The wide availability of computers now allows one to simulate the full transport process in order to avoid the limitations of the box model. The effects of the electric field inside the insulator on the high energy electrons is now included. The simulation provides a method to experimentally determine the dependence of secondary electron emission on electric field strength at the surface of insulators. The occurrence of partial discharges has been correlated with the development of internal spacecharge fields. The rate of spontaneous partial discharge pulses in spacecraft insulation has been correlated with the flux of fast electrons from space. Spacecraft surface voltage also correlates with fast electron flux. Partial discharges at the surface of irradiated insulators in vacuum are associated

with a burst of gas which modifies or controls the surface discharge process. Perhaps the gas results from the Lichtenberg figure noted by Gross. The conditions for violation of the integrity of glass envelopes by electron bombardment of high voltage electron tubes have been investigated. Improved Compton Diodes have resulted from detailed studies of the currents in irradiated complex material structures.

The works of Gross have helped to point us towards the future. The analysis of normal-incidence one-dimensional problems has been successful and encourages one to confidently attempt three dimensional problems. The conditions that allow radiation to cause full insulator breakdown are being enumerated with increasing clarity. The nature of spontaneous discharge pulses is being determined. Knowledge of radiation effects in semiconductors is beginning to assist in the understanding of insulator effects. The detailed delineation of fast electron transport and stopping now allows one to experimentally address the issue of conduction currents with more clarity.

References

1. B. Gross, Topics in Applied Physics **33**:Electrets, 217 (1979).
2. B. Gross, *Charge Storage in Dielectrics, a Bibliographical Review on the Electret and Related Effects*, Elsevier, Amsterdam, 1964.
3. B. Gross, Physical Review **107**(2), 368 (1957).
4. B. Gross, Solid State Communications **15**, 1655 (1974).
5. B. Gross, J. Polymer Science **27**, 135 (1958).
6. B. Gross, Z. Physik **155**, 479 (1959).
7. B. Gross, IEEE Trans. Nuclear Science **25**(4), 1048 (1978).
8. B. Hess, Z. Angew. Physik **11**, 449 (1959).
9. L. Nunes de Oliveira and B. Gross, J. Appl. Phys. **46**(7), 3132 (1975).
10. B. Gross, G. M. Sessler and J. E. West, J. Appl. Phys. **45**, 2840 (1974).
11. B. Gross and G. F. Leal Ferreira, J. Appl. Phys. **50** (3), 1506 (1979).
12. A. R. Frederickson, *Radiation-induced Electrical Current and Voltage in Dielectric Structures,* AFCRL-TR-74-0582 (1974).
13. A. R. Frederickson, IEEE Trans. Nuc. Sci. **22**, 2556 (1975).
14. S. Matsuoka, H. Sunaga, R. Tanaka, H. Hagiwara and K. Araki, IEEE Trans. Nuc. Sci. **23**, 1447-52 (1976).
15. J. Pigneret and H. Strobeck, IEEE Trans. Nuc. Sci. **23**, 1886 (1976).
16. D. A. Berkeley, J. Appl. Phys. **50**, 3447 (1979).
17. B. Gross, A. Bradley and A. P. Pinkerton, J. Appl. Phys. **31** (6), 1035 (1960).
18. M. J. Berger, Radiation Research **12** (4), 422 (1960). J. Appl. Phys. **28** (12), 1502 (1957).
19. B. Gross, R. Gerhard-Multhaupt, K. Labonte and A. Berraissoul, Colloid & Polymer Science **262**, 93-98 (1984).
20. T. Tabata, P. Andreo and R. Ito, Nuclear Instruments and Methods B**94**, 103 (1994).
21. J. A. Halbleib, R. P. Kensek, G. Valdez, S. M. Seltzer and M. J. Berger, IEEE Trans. Nuc. Sci. **39,** 1025 (1992).
22. A. R. Frederickson, J. T. Bell and E. A. Beidl, IEEE Trans. Nuc. Sci. **42**, 1910 (1995).
23. B. Gross and S. V. Nablo, J. Appl. Phys. **38** (5), 2272 (1967).
24. B. Gross, J. Dow and S. V. Nablo, J. Appl. Phys. **44** (6), 2459 (1973).
25. A. R. Frederickson and S. Woolf, IEEE Trans. Nuc. Sci. **29** (6), 2004 (1982).
26. R. Gerhard-Multhaupt, Phys. Rev. B**27**, 2494 (1983).
27. M. Hikita, M. Zahn, K. A. Wright, C. M. Cooke and J. Brennan, IEEE Trans. Electrical Insulation **23**, 861 (1988).
28. A. R. Frederickson, S. Woolf and J. C. Garth, IEEE Trans. Nuc. Sci. **40** (6), 1393 (1993).
29. B. Gross and M. M. Perlman, J. Appl. Phys. **43**, 853-7 (1972).
30. W. Shockley, J. Appl. Phys. **9**, 635 (1938). This is derived for slowly varying currents where Maxwell's first equation, $\mathbf{div\,D=Q}$, alone suffices.
31. A. R. Frederickson, Proceedings, 17 th International Symposium on Discharges and Electrical Insulation in Vacuum, Berkeley, CA, 517-22, July, 1996. Sponsored by IEEE and APS.
32. A. R. Frederickson, IEEE Trans. Elec. Insul. **18**, 337 (1983).
33. K. G. Balmain and G. R. Dubois, IEEE Trans. Nuc. Sci. **26**, 5146 (1979).
34. A. R. Frederickson, L. Levy and C. L. Enloe, IEEE Trans Elec. Insul. **27** (6), 1166 (1992).
35. A. R. Frederickson, IEEE Trans. Nuc. Sci. **43** (2), 426 (1996).
36. E. P. Wenaas, M. J. Treadaway, T. M. Flanagan, C. E. Mallon and R. Denson, IEEE Trans. Nuc. Sci. **26**, 5152 (1979).
37. M. D. Violet and A. R. Frederickson, IEEE Trans. Nuc. Sci. **40**, 1512 (1993).
38. A. R. Frederickson, E. G. Holeman and E. G.

Mullen, IEEE Trans. Nuc. Sci. **39**, 1773 (1992).
39. A. R. Frederickson, IEEE Trans. Nuc. Sci. **43**, 2778 (1996).
40. A. R. Frederickson, *Proceedings of 1981 Conference on Electrical Insulation and Dielectric Phenomena*, 45-51, (1981) IEEE Publication 81-CH1668-3.
41. H. B. Garrett, Rev. Geophysics Space Physics **19**, 577 (1981).
42. E. C. Whipple, Reports on Progress in Physics **44**, 1197 (1981).
43. B. Gross, H. von Seggern and A. Berraissoul, Proc. Fifth Intern. Symp. Electrets, Heidelberg, 608 (1985).
44. E. G. Mullen, A. R. Frederickson, G. P. Murphy, K. P. Ray and E. G. Holeman, IEEE Trans. Nuc. Sci. **44** (6), 2188 (1997).
45. G. Wrenn, J. Spacecraft Rockets **32** (3), 514 (1995).
46. C. K. Purvis, H. B. Garrett, A. C. Whittlesey and N. J. Stevens, *Design guidelines for Assessing and Controlling Spacecraft Charging Effects,* NASA Technical Paper 2361 (1984).
47. V. D. Bochkov, Proceedings 17 th International Symposium on Discharges and Electrical Insulation in Vacuum, Berkeley, CA, 517-22 (July, 1996). Sponsored by IEEE and APS. Also, "Investigation of Dielectric Strength of Vacuum Electronic Devices Operating Above 50 kV....." PhD Dissertation, Ryazan Radioengineering Institute, Ryazan, Russia (1982).
48. A. R. Frederickson and A. D. Morris, *U. S. Letters Patent 3,780,304* "Charge Accumulation Gamma Radiation Detector" (18 December 1973).
49. Private Correspondence, Dale Ferguson and David Snyder, NASA Lewis Research Center, Cleveland, Ohio, USA, September, 1997.
50. A. R. Frederickson, IEEE Trans. Nuc. Sci. **36** (6), 2405 (1989).
51. A. R. Frederickson, P. B. McGrath and P. Leung, Proceedings, 1989 Conference on Electrical Insulation and Dielectric Phenomena, 210-17, IEEE #89CH2773-0 (1989).
52. B. Gross and P. Gunther, IEEE Trans. Nuc. Sci. **40**, 83 (1993).
53. A. R. Frederickson, *Proceedings Symposium on Spacecraft Materials in Space Environment,* 221-31, ONERA-CERT, Toulouse, France (September, 1988).
54. L. Nunes de Oliveira and G. F. Leal Ferriera, Phys. Rev. B**11** (6), 2311 (1975).
55. A. R. Frederickson, IEEE Trans. Nuc. Sci. **40**, 1547 (1994).

The following papers by Gross and co-workers are helpful, especially for conductivity.

B. Gross and R. Hessel, IEEE Trans. Elec. Insul. **26**(1), 18 (1991).

B. Gross, R. Gerhard-Multhaupt, A. Berraissoul and G. M. Sessler, J. Appl. Phys. **62**(4), 1429 (1987).

R. G. Filho, B. Gross and R. M. Faria, IEEE Trans. on Electrical Insulation EI- **21**(3), 431 (1986).

B. Gross, H. Von Seggern, R. Gerhard-Multhaupt, J. Phys. D Appl. Phys. **18**, 2497 (1985).

B. Gross, H. Von Seggern, and J. E. West, J. App. Phys. **58**(8), 2333 (1984).

R. M. Faria, B. Gross, and R. G. Filho, IEEE Conf. On Electrical Insulation and Dielectric Phenomena, Clayton, DE, October 21-24, 1984.

B. Gross, H. von Seggern and D. A. Berkley, Phys. Stat. Sol. (A)**79**, 607 1983.

B. Gross, J. A. Giacometti and G. F. Leal Ferreira, IEEE Trans. on Nuclear Science **28**, (1981).

B. Gross, IEEE Conf. On Electrical Insulation and Dielectric Phenomena, Pocono Manor, Pennsylvania, Oct.-Nov. 1978.

B. Gross, J. Electrostatics **1**, 125 (1975).

B. Gross and L. Nunes de Oliveira, J. Appl. Phys. **45**(10), 4724 (1974).

B. Gross, G. M. Sessler and J. E. West, Appl. Phys. Lett. **24**(8), 351 (1974).

B. Gross, G. M. Sessler and J. E. West, Appl. Phys. Lett. **22**(7), 315 (1973).

B. Gross, Zeit. Angew. Phys. **30**(5), 323 (1971).

B. Gross, J. Appl. Phys. **36**(5), 1635 (1965).

P V. Murphy and B. Gross, J. Appl. Phys. **35**(1), 171 (1964).

P V. Murphy, S. Costa Ribeiro, F. Milanez and R. J. De Moraes, J. Chem. Phys. **38**(10), 2400 (1963).

B. Gross and R. J. De Moraes, J. of Chem. Phys. **37**(4), 710 (1962).

B. Gross, Zeit. Phys. **155**, 479 (1959).